J|A|C|S
ARTICLES

Published on Web 02/04/2009

Stable "Inverse" Sandwich Complex with Unprecedented Organocalcium(I): Crystal Structures of $[(thf)_2Mg(Br)\text{-}C_6H_2\text{-}2,4,6\text{-}Ph_3]$ and $[(thf)_3Ca\{\mu\text{-}C_6H_3\text{-}1,3,5\text{-}Ph_3\}Ca(thf)_3]$

Sven Krieck,[†] Helmar Görls,[†] Lian Yu,[‡] Markus Reiher,*[,‡] and Matthias Westerhausen*[,†]

Institute of Inorganic and Analytical Chemistry, Friedrich-Schiller-Universität Jena, August-Bebel-Strasse 2, D-07743 Jena, Germany, and Laboratorium für Physikalische Chemie, ETH Zurich, Hönggerberg Campus, Wolfgang-Pauli-Strasse 10, CH-8093 Zurich, Switzerland

Received November 4, 2008; E-mail: markus.reiher@phys.chem.ethz.ch (M.R.); m.we@uni-jena.de (M.W.)

Abstract: The reaction of bromo-2,4,6-triphenylbenzene with activated magnesium in THF yielded the Grignard reagent $[(thf)_2Mg(Br)\text{-}C_6H_2\text{-}2,4,6\text{-}Ph_3]$ (**1**) with a Mg−C bond length of 214.8(3) pm. A similar reaction of bromo-2,4,6-triphenylbenzene with activated calcium led to an "inverse" sandwich complex $[(thf)_3Ca\{\mu\text{-}C_6H_3\text{-}1,3,5\text{-}Ph_3\}Ca(thf)_3]$ (**2**) with the calcium atoms on opposite sides of the central arene ring showing small Ca−Ca′ and Ca−C distances of 427.9(3) and 259.2(3) pm. This extremely air- and moisture-sensitive complex exhibits thermochomic and solvatochromic behavior. It is paramagnetic with spin of $S = 1$ (triplet) with an ESR resonance at $g = 2.0023$. Quantum chemical calculations shed light on the bonding situation in this very unusual dinuclear Ca(I) compound.

Introduction

Calcium is one of the most widespread metals on earth, and in all its compounds calcium is considered as redox-inert and always exhibits the oxidation state +2. Similar considerations are valid for the other alkaline earth metals, as well as for zinc and cadmium. However, extremely sophisticated procedures allowed the identification of metal(I) species. The insertion of Zn or Mg atoms into a M−Cl bond of MCl_2 yielding ClM−MCl could be achieved in an equilibrium at high temperatures.[1] Also, extremely reactive molecules H−M−M−H were generated via the reaction of Mg[2] or Ca[3] with hydrogen but had to be trapped in an extremely cold matrix preventing intermolecular degradation. Very recently, Carmona and co-workers prepared an organometallic Zn(I) compound, [Cp*Zn−ZnCp*] with a stable Zn−Zn bond.[4] The stabilization of the Zn_2^{2+} fragment succeeded also with other bulky substituents[5,6] which allowed the isolation of the homologous Cd(I) derivative, too.[7] Even more remarkable, shielding of the reactive metal−metal bond by bulky groups facilitated the synthesis of the surprisingly stable Mg(I) compounds, XMg−MgX, with Mg(I)−Mg(I) bonds.[8] With X as a bulky *N*,*N*′-diaryl-1,3-diketiminate ligand decomposition occurred only above 300 °C and this compound was sublimed at 230 °C and 10^{-6} mm Hg. Quantum chemical investigations showed that beryllium(I) compounds should be much more feasible than calcium(I) derivatives.[9] Nevertheless, large groups should also be able to stabilize Ca(I)−Ca(I) bonds.[10,11] However, aryl ligands could cause side reactions due to the competition between σ- and π-interactions of the soft calcium(I) atom with the aryl groups. In all these reactions yielding Zn(I), Mg(I), and Ca(I) compounds, the atomization energies of the metals (Zn, 114.2; Mg, 127.6; Ca, 150.6 kJ mol^{-1}) have to be overcome before one can profit from the exothermic reaction enthalpies. Thus, monomeric methylcalcium(I),[12,13] cyclopentadienylcalcium(I),[13] and ethynylcalcium(I) radicals[14] were prepared from calcium atoms and organic precursors in the gas phase and identified by laser excitation spectroscopy.

In principle two reaction pathways can be thought of in order to stabilize molecular calcium(I) compounds. On the one hand, the formation of Ca−Ca bonds should yield stable molecules with calcium(I) atoms[10,11] as was also performed earlier for magnesium[8] and zinc.[4−6] Bulky groups are necessary in order to sterically shield the reactive metal−metal bond. The Ca−Ca

[†] Friedrich-Schiller-Universität Jena.
[‡] ETH Zurich.

(1) Krumpelt, M.; Fischer, J.; Johnson, I. *J. Phys. Chem.* **1986**, *72*, 506–510.
(2) Jasien, P. G.; Dykstra, C. E. *J. Am. Chem. Soc.* **1985**, *107*, 1891–1895.
(3) Xiao, Z. L.; Hauge, R. H. *High Temp. Sci.* **1991**, *31*, 59–77.
(4) Resa, I.; Carmona, E.; Gutierrez-Puebla, E. A. Monge *Science* **2004**, *305*, 1136–1138.
(5) Zhu, Z.; Wright, R. J.; Olmstead, M. M.; Rivard, E.; Brynda, M.; Power, P. P. *Angew. Chem.* **2006**, *118*, 5939–5942. *Angew. Chem., Int. Ed.* 2006, *45*, 5807−5810.
(6) Wang, Y.; Quillian, B.; Wei, P.; Wang, H.; Yang, X.-J.; Xie, Y.; King, R. B.; Schleyer, P.v.R.; Schaefer, H. F.; Robinson, G. H. *J. Am. Chem. Soc.* **2005**, *127*, 11944–11945.
(7) Zhu, Z.; Fischer, R. C.; Fettinger, J. C.; Rivard, E.; Brynda, M.; Power, P. P. *J. Am. Chem. Soc.* **2006**, *128*, 15068–15069.
(8) Green, S. P.; Jones, C.; Stasch, A. *Science* **2007**, *318*, 1754–1757.
(9) Velazquez, A.; Fernández, I.; Frenking, G.; Merino, G. *Organometallics* **2007**, *26*, 4731–4736.
(10) Westerhausen, M; Gärtner, M.; Fischer, R.; Langer, J.; Yu, L.; Reiher, M. *Chem. Eur. J.* **2007**, *13*, 6292–6306.
(11) Westerhausen, M. *Angew. Chem.* **2008**, *120*, 2215–2217; *Angew. Chem., Int. Ed.* **2008**, *47*, 2185−2187.
(12) Brazier, C. R.; Bernath, P. F. *J. Chem. Phys.* **1987**, *86*, 5918–5922.
(13) Ellis, A. M.; Robles, E. S. J.; Miller, T. A. *J. Chem. Phys.* **1991**, *94*, 1752–1758.
(14) Bopegedera, A.M.R.P.; Brazier, C. R.; Bernath, P. F. *J. Mol. Spectrosc.* **1988**, *129*, 268–275.

bond energy was expected at a value of 105 kJ mol^{-1}.[15] On the other hand, the ionization energies of the first and second ionization of calcium giving Ca^+ and Ca^{2+}, respectively, differ significantly with values of 6.11 and 11.87 eV.[15] Offering an arene with a π^* orbital between these two ionization potentials should offer the possibility to stabilize calcium(I) complexes. Coordination of two metal atoms on opposite sides of the arene leads to the formation of quite unusual "inverse" sandwich complexes, a concept which was applied in order to stabilize low oxidation states of the elements of the boron group such as $[M(\mu,\eta^5\text{-}C_5Me_5)M]^+$ (M = Ga,[16] In[17]). Recent quantum chemical calculations also corroborated the particular stability of such "inverse" sandwich cations.[18]

The reduction of anthracene with alkaline earth metals was already studied in detail by Bogdanović and others[19,20] in order to activate the alkaline earth metals. Anthracene reacted with magnesium to form [tris(tetrahydrofuran)magnesium anthracene] and decomposed at elevated temperatures yielding anthracene and highly activated and pyrophoric magnesium powder.[21] In order to activate the magnesium pieces, addition of small amounts of bromoethane might be necessary.[22] A similar reaction of calcium with anthracene led to the formation of [tetrakis(tetrahydrofuran)calcium anthracene].[23] The transmetalation of [tris(tetrahydrofuran)magnesium anthracene] offers another access route to this calcium−arene complex. In very concentrated anthracene solutions violet [hexakis(tetrahydrofuran)calcium bis(anthracene)] forms which decomposes to anthracene and the above-mentioned calcium complex upon dilution.[23]

Results and Disscussion

Synthesis. We are investigating the direct synthesis of heavy Grignard reagents of the type Aryl−Ca−X from the insertion of activated calcium into C−X bonds (X = Br, I) of halogenoarenes.[24−26] These arylcalcium halides are extremely sensitive toward air and moisture and easily cleave ether.[27,28] Substituents in the ortho position often cause severe challenges:

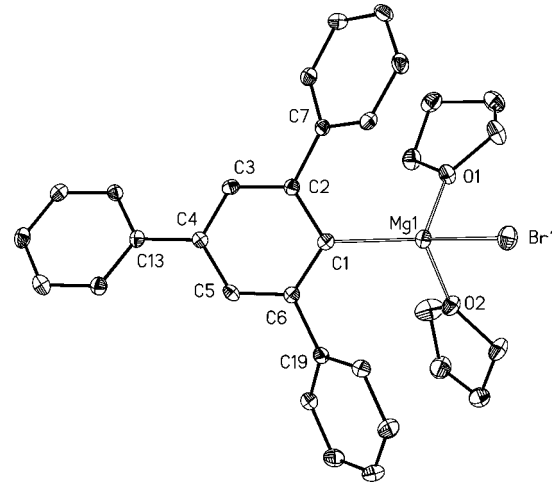

Figure 1. Representation of molecular structure and numbering scheme of $[(thf)_2Mg(Br)\text{-}C_6H_2\text{-}2,4,6\text{-}Ph_3]$ (**1**). The ellipsoids represent a probability of 40%. H atoms are omitted for the sake of clarity. Selected bond lengths (pm): Mg1−Br1 246.83(9), Mg1−C1 214.8(3), Mg1−O1 204.3(2), Mg1−O2 203.1(2), C1−C2 142.1(3), C1−C6 141.6(4), C2−C3 140.4(4), C3−C4 139.4(4), C4−C5 139.0(3), C5−C6 139.9(3), C2−C7 149.3(4), C4−C13 149.2(3), C6−C19 149.6(3); angles (deg): Br1−Mg1−C1 129.00(8), Br1−Mg1−O1 104.89(6), Br1−Mg1−O2 101.92(6), C1−Mg1−O1 110.23(9), C1−Mg1−O2 110.2(1), O1−Mg1−O2 95.23(8), Mg1−C1−C2 120.5(2), Mg1−C1−C6 123.6(2), C2−C1−C6 114.8(2).

halogen atoms are not tolerated and methyl groups can be metallated leading to benzyl derivatives. Here we investigate the reaction of 1-bromo-2,4,6-triphenylbenzene with activated magnesium and calcium metal. Colorless $[(Et_2O)_2Li\text{-}C_6H_2\text{-}2,4,6\text{-}Ph_3]$ was already accessible via metal−halogen exchange[29,30] and reacts with CuBr in the presence of dimethylsulfane to the corresponding colorless copper derivative $[(Me_2S)Cu\text{-}C_6H_2\text{-}2,4,6\text{-}Ph_3]$.[31]

The insertion of magnesium into the C−Br bond of 1-bromo-2,4,6-triphenylbenzene yielded $[(thf)_2Mg(Br)\text{-}C_6H_2\text{-}2,4,6\text{-}Ph_3]$ (**1**) with a tetra-coordinate magnesium atom according to eq 1. Cooling of a concentrated reaction solution led to precipitation of colorless needles of **1** with a melting point of 165 °C.

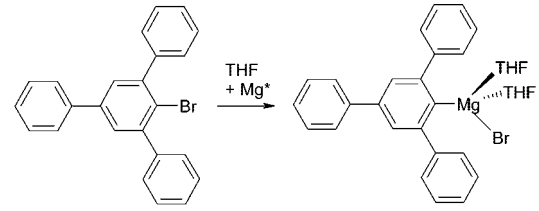

(1)

Molecular structure and numbering scheme of **1** are represented in Figure 1. The Mg1−C1 bond length of 214.8(3) pm and the Mg1−O distances of 203.1(2) and 204.3(2) pm lie in characteristic regions.[32−34] The endocyclic C2−C1−C6 angle is extremely small and shows a value of 114.8(2)°. Even smaller values of 111.8(6)° were found for $[(Et_2O)_2Li\text{-}C_6H_2\text{-}2,4,6\text{-}Ph_3]$.[29,30] These rather low internal ring angles are characteristic for mainly ionic metal−carbon interactions to aryl groups due to electro-

(15) Holleman, A. F.; Wiberg, E.; Wiberg N. *Lehrbuch der Anorganischen Chemie (Holleman-Wiberg)*, 102nd ed.; Walter de Gruyter: Berlin, 2007.
(16) Buchin, C.; Gemel, C.; Cadenbach, T.; Schmid, R.; Fischer, R. A. *Angew. Chem.* **2006**, *118*, 1091–1093; *Angew. Chem., Int. Ed.* **2006**, *45*, 1074−1076. Corrigendum: *Angew. Chem.* **2006**, *118*, 1703; *Angew. Chem., Int. Ed.* **2006**, *45*, 1674.
(17) Jones, J. N.; Macdonald, C. L. B.; Gorden, J. D.; Cowley, A. H. *J. Organomet. Chem.* **2003**, *666*, 3–5. (a) See also Dagorne, S.; Atwood, D. A. *Chem. Rev.* **2008**, *108*, 4037–4071.
(18) Fernández, I.; Cerpa, E.; Merino, G.; Frenking, G. *Organometallics* **2008**, *27*, 1106–1111.
(19) Bogdanović, B. *Acc. Chem. Res.* **1988**, *21*, 261–267.
(20) Aleandri, L. E.; Bogdanović, B. *Active Met.* **1996**, 299–338.
(21) Bartmann, E.; Bogdanović, B.; Janke, N.; Liao, S.; Schlichte, K.; Spliethoff, B.; Treber, J.; Westeppe, U.; Wilczok, U. *Chem. Ber.* **1990**, *123*, 1517–1528.
(22) Bogdanović, B.; Janke, N.; Krüger, C.; Mynott, R.; Schlichte, K.; Westeppe, U. *Angew. Chem.* **1985**, *97*, 972–974; *Angew. Chem., Int. Ed. Engl.* **1985**, *24*, 960−962.
(23) Bönnemann, H.; Bogdanović, B.; Brinkmann, R.; Egeler, N.; Benn, R.; Topalovic, I.; Seevogel, K. *Main Group Met. Chem.* **1990**, *13*, 341–362.
(24) Fischer, R.; Gärtner, M.; Görls, H.; Yu, L.; Reiher, M.; Westerhausen, M. *Angew. Chem.* **2007**, *119*, 1642–1647; *Angew. Chem., Int. Ed.* **2007**, *46*, 1618−1623.
(25) Westerhausen, M; Gärtner, M.; Fischer, R.; Langer, J. *Angew. Chem.* **2007**, *119*, 1994–2001; *Angew. Chem., Int. Ed.* **2007**, *46*, 1950−1956.
(26) Westerhausen, M. *Coord. Chem. Rev.* **2008**, *252*, 1516–1531.
(27) Gärtner, M.; Görls, H.; Westerhausen, M. *Synthesis* **2007**, 725–730.
(28) Gärtner, M.; Görls, H.; Westerhausen, M. *J. Organomet. Chem.* **2008**, *693*, 221–227.
(29) Olmstead, M. M.; Power, P. P. *J. Organomet. Chem.* **1991**, *408*, 1–6.
(30) Girolami, G. S.; Riehl, M. E.; Suslick, K. S.; Wilson, S. R. *Organometallics* **1992**, *11*, 3907–3910.
(31) He, X.; Olmstead, M. M.; Power, P. P. *J. Am. Chem. Soc.* **1992**, *114*, 9668–9670.

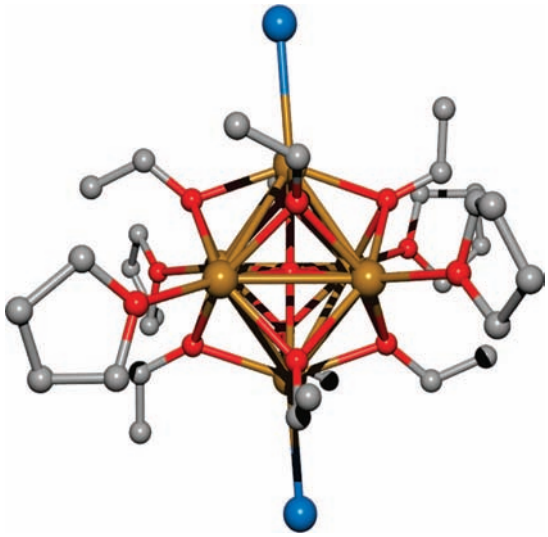

Figure 2. Molecular structure of the complex [{(thf)Ca(O−CH═CH_2)$_2$}$_4$·CaO·CaI_2]. The vinylate anions are located above the Ca_3 faces of the oxygen-centered Ca_6 octahedron (Ca gold, O red, C gray; Ca−O_{cent} 232.8(1), 230.4(1) and 230.1(1) pm; Ca−$O_{vinylate}$ 236.3(5)−240.0(5) pm). At opposite edges the iodide ions (blue) are bound (Ca1−I1 306.9(1) pm) and the other calcium atoms are coordinated to THF molecules (Ca−O_{THF} 239.4(6) and 239.2(5) pm).

static repulsion between the anionic sp^2 electron pair and the neighboring C−C bonds.[35]

The insertion of calcium into C−X bonds of halogenoarenes succeeds at low temperatures. Iodo- and bromobenzene react readily with activated calcium, whereas only mesityliodide (1-iodo-2,4,6-trimethylbenzene) is able to form the Grignard reagent from the direct synthesis with calcium powder. A large variety of functional groups is tolerated in the para position, the phenyl substituent being an exception. The choice of ortho substituents, however, is limited due to degradation reactions.[27] The fast degradation of 4-phenylphenylcalcium halides[27] and the stability of bis[2,4,6-triphenylphenylcalcium(I)] according to quantum chemical investigations[10] inspired us to investigate the reaction of 1,3,5-triphenylbenzene with calcium powder.

The reaction of 1-bromo-2,4,6-triphenylbenzene with an excess of activated calcium in tetrahydrofuran (THF) at −60 °C yielded unexpectedly [$(thf)_3Ca\{\mu$-$Ph_3C_6H_3\}Ca(thf)_3$] (**2**). If this reaction is performed in a sealed NMR tube, the formation of ethene and vinylalkoholate was also observed as byproduct due to ether cleavage reactions of intermediate 2,4,6-$Ph_3C_6H_2$-CaBr. NMR studies of the mother liquor showed the existence of stoichiometric amounts (in relation to tpb) of the vinylate anion H_2C═CH_2−O^-.[36] The reaction of activated calcium with bromo-2,4,6-triphenylbenzene in [D_8]THF gave monodeuterated triphenylbenzene anions in **2** confirming that the first reaction step consists of a direct synthesis (insertion of Ca into the C−Br bond, formation of a heavy Grignard reagent), followed by an ether cleavage reaction and reduction by the excess of activated calcium metal. THF cleavage is a common degradation reaction for heavy Grignard reagents.[27,36−39] With knowledge of the molecular structure of **2** we also tried to prepare this complex from activated calcium and 1,3,5-triphenylbenzene (tpb = 1,3,5-$Ph_3C_6H_3$) in THF; however, no reaction occurred. After addition of catalytic amounts of 2,4,6-$Ph_3C_6H_2$-Br the reaction was initiated and **2** formed with good yield, as shown in eq 2.

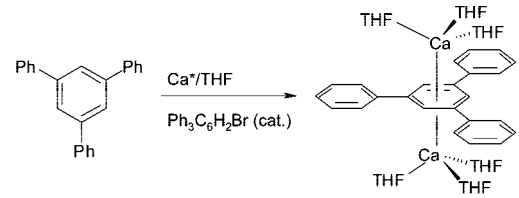

(2)

A major aspect is guaranteeing the absence of anions other than the tpb^{2-} anion. In order to exclude anions such as hydride, bromide, oxide, and vinylate, derivatization reactions were performed.

(i) Absence of hydride: Solid state ^{1}H NMR experiments showed no resonances below δ = 0 ppm and, hence, allowed the exclusion of additional hydride in compound **2**. In addition, the reaction of **2** with D_2O or [D_4]methanol gave D_2; however, neither H_2 nor HD were detected. Furthermore, neither deuterated triphenylbenzene nor deuterated hexahydrobenzene species were present.

(ii) Absence of vinylate: The NMR spectrum of the reaction solution showed the formation of H_2C═CH−O^- anions due to ether cleavage. Crystalline **2** was dissolved in [D_8]THF, and the ^{1}H and ^{13}C {^{1}H} NMR spectra only showed the resonances of triphenylbenzene and THF, the presence of vinylalkoholate anions could safely be excluded. The reaction of **2** with excess of chloro-trimethylsilane and the characterization via GC-MS techniques showed Cl−$SiMe_3$ (excess), triphenylbenzene, THF, and benzene; however, vinyl-trimethylsilylether was absent. The validity of the applied analytical methods was controlled via repetition of the derivatization reactions with [{(thf)Ca(O−CH═CH_2)$_2$}$_4$·CaO·CaI_2] (**3**) which was obtained by a zinc-mediated degradation of an organocalcium solution in THF.[40] Compound **3** is shown in Figure 2 and can be described as an oxygen-centered Ca_6 octahedron. The vinylate anions are located above all faces, the iodide anions bind to two opposite calcium

(32) Markies, P. R.; Akkerman, O. S.; Bickelhaupt, F.; Smeets, W. J. J.; Spek, A. L. *Adv. Organomet. Chem.* **1991**, *32*, 147–226.
(33) Holloway, C. E.; Melnik, M. *J. Organomet. Chem.* **1994**, *465*, 1–63.
(34) Bickelhaupt, F. in Richey, G. H. (ed.): *Grignard Reagents: New Developments*; Wiley: Chichester, 2000; Chapter 9, pp 299−328.
(35) Maetzke, T.; Seebach, D. *Helv. Chim. Acta* **1989**, *72*, 624–630.
(36) NMR data of vinylalcoholate species: ^{1}H NMR ([D_8]THF, 400.25 MHz, 300 K, signals are verified with H, H-COSY experiments): δ 6.83 (1H, d, J_{gem} = 6.4 Hz, CH_2), 7.12 (2H, dd, J_{gem} = 7.6 Hz, J_{trans} = 6.8 Hz, CH_2), 8.29 (1H, d, J_{trans} = 5.8 Hz, CH−O). 13C{^{1}H} NMR ([D_8]THF, 50.32 MHz, 300 K): δ 126.8 (1C, *C*H_2), 150.3 (1C, CH−O); similar values were observed during degradation of arylcalcium iodides in THF solution:(a) Fischer, R.; Gärtner, M.; Görls, H.; Westerhausen, M *Organometallics* **2006**, *25*, 3496–3500.
(37) Fischer, R.; Görls, H.; Westerhausen, M. *Inorg. Chem. Commun.* **2005**, *8*, 1159–1161.
(38) Fischer, R.; Gärtner, M; Görls, H.; Westerhausen, M. *Angew. Chem.* **2006**, *118*, 624–627. (a) *Angew. Chem., Int. Ed.* **2006**, *45*, 609−612.
(39) Gärtner, M.; Görls, H.; Westerhausen, M. *J. Organomet. Chem.* **2008**, *693*, 221–227.
(40) Krieck, S.; Westerhausen, M.,unpublished results. This compound was obtained with good yield during the attempt to transmetallate alkylzinc compounds in THF solution. ^{1}H NMR data: δ 6.15 (dd, ^3J(H, H)$_{trans}$ = 14.0 Hz, ^3J(H, H)$_{cis}$ = 6.2 Hz), 3.83 (d, ^3J(H, H)$_{trans}$ = 13.9 Hz), 3.39 (d, ^3J(H, H)$_{cis}$ = 6.2 Hz); ^{13}C NMR data: δ 68.7, 91.5; IR: 1615 (C═C), 963 (O−C═C), 887 and 1035 (C−O−C, THF). These data are in agreement with literature values of vinylate anions: (a) Basuli, F.; Tomaszewski, T.; Huffman, J. C.; Mindiola, D. J. *Organometallics* **2003**, *22*, 4705–4714. (b) Evans, W. J.; Dominguez, R.; Hanusa, T. P. *Organometallics* **1986**, *5*, 1291–1296. (c) Thiele, K.-H.; Unverhau, K.; Geitner, M.; Jacob, K. *Z. Anorg. Allg. Chem.* **1987**, *548*, 175–179.

atoms. All other calcium atoms complete their coordination spheres by THF ligands.

(iii) The absence of bromide can be deduced from the structure determination and from the fact that catalytic amounts of 2,4,6-$Ph_3C_6H_2$-Br are sufficient in order to prepare **2** nearly quantitatively.

(iv) Absence of oxide anions: Due to the extremely strong basicity of oxide anions, these bases cannot be situated in gaps between molecules but have to be surrounded by metal cations (leading to the formation of oxygen-centered cage compounds).[41−45] The X-ray structure analysis gave no hints on the presence of other anions in the solid state.

(v) The "inverse" sandwich complex **2** with Ca(I) atoms is surprisingly unreactive toward ether and exhibits no tendency to cleave ether. This fact is in agreement with the observation that also magnesium(I) compounds are able to coordinate THF molecules and to form THF adducts without destroying the Mg−Mg bond.[46] However, in these diamagnetic Mg(I) compounds a totally different bonding situation is found. Compound **2** exhibits strong reducing properties but due to charge delocalization the Lewis basicity (and hence nucleophilicity) of tpb^{2-} is rather weak.

Hence, the presence of other anions is excluded on the basis of derivatization reactions and spectroscopic measurements. The determination of the calcium content (ICP-OES) verified the constitution. However, due to extreme sensitivity of **2** toward moisture and air and due to the fact that the mass changed during handling and weighing (loss of THF), an elemental analysis gave unreliable results.

Structural Characterization of the Inverse Sandwich 2. Complex **2** was recrystallized from THF at −40 °C giving black crystals suitable for X-ray crystallography. The quality of the crystal structure is hampered due to thermal motion and disordering of the THF ligands, and hence, we complemented the experimental results by dispersion-corrected quantum chemical calculations (B97-D,[47] see the Computational Methodology below). The molecular structure of this black compound **2** is presented in Figure 3. The central structural fragment consists of a strictly planar 1,3,5-triphenylbenzene anion with two $(thf)_3Ca$ moieties bound to the arene. The calcium atoms lie on a C_3-like axis and are located above and below the center of the inner arene ring yielding an "inverse" sandwich complex with the arene *between* the two metal cations. Small Ca−Ca′ and Ca−C distances of 427.9(3) and 259.2(3) pm, respectively, are observed. The distance between the calcium atoms and the center of the inner arene ring of **2** (214 pm) is significantly smaller than the calculated values of Ca^+ (263.6 pm)[48] and Ca^{2+} (280−290 pm dependent on the number of additional water ligands)[49] to the π-system of benzene. This strong interaction also affects the structural parameters of the tpb^{2-} anion: On the one hand, the reduction of this molecule in **2** leads to elongation of the C−C bonds of the inner arene ring (146.4 pm) in comparison to free 1,3,5-triphenylbenzene with a propeller-like arrangement (tpb: 138.7 pm).[50] On the other hand, the ring−ring C−C distances of **2** (143.5 pm) are somewhat smaller than those of neutral tpb (148.7 pm).[50]

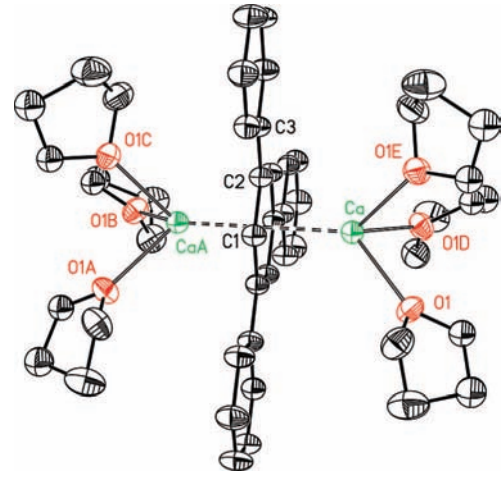

Figure 3. Numbering scheme and molecular structure of **2** (Ca green, O red, C black). Symmetry-related atoms are marked with the letters "A" (x, y, $-z + 0.5$), "B" ($-y + 1$, $x - y$, z), and "C" ($-x + y + 1$, $-x + 1$, z). The ellipsoids represent a probability of 40%, disordering of THF ligands and H atoms are neglected for clarity reasons. Selected bond lengths (pm): Ca−O1 240.5(3), Ca−C1 258.6(3), Ca−C2 259.8(3), Ca···CaA 427.9(3), C1−C2 147.8(7), C1−C2B 144.9(7), C2−C3 143.5(7); angles (deg): O1−Ca−O1B 84.4(1), C2−C1−C2B 121.4(5), C1−C2−C1C 118.6(5).

In order to understand the experimental results, it was necessary to perform quantum chemical calculations. It can easily be anticipated that structure and stability of complex **2** are also governed by dispersion interactions that cannot be handled with standard methods of density functional theory (DFT). Desirable coupled-cluster calculations within the CCSD(T) model are unfeasible because of the size of the system comprising two Ca atoms, a large organic ligand, and six THF solvent molecules. Consequently, we tackled this problem by a combined second-order Møller−Plesset (MP2) and dispersion-corrected DFT approach. The dispersion correction was included semiempirically as proposed and implemented by Grimme.[47] It should be noted, however, that the MP2 structure optimization for the triplet state was difficult to converge in terms of the length of the geometric gradient of the electronic energy.

An important issue regarding the accuracy is the reliability of the DFT methods. Although MP2 calculations have only been feasible for a simplified model system stripped by all six THF solvent molecules, namely for Ca−tpb−Ca, this small model allowed us to employ the large TZVPP basis set. We found that B97-D produces an equilibrium Ca−Ca distance for the triplet state of 432.6 pm, which is up to 20 pm larger than the ones optimized with BP86, B3LYP, and TPSS. Interestingly, the optimized quintet state, which is 77 kJ/mol (B97-D) above the triplet structure, turned out to yield similar results for all methods (MP2, 452 pm; B97-D, 453 pm; BP86, 450 pm; B3LYP, 454 pm; TPSS, 446 pm). Moreover, the closed-shell singlet for the solvent-free Ca−tpb−Ca model is about 61 kJ/mol (B97-D/TZVPP) above the triplet state and features an almost doubled Ca−Ca distance (compared to the triplet

(41) Turova, N. Y.; Turevskaya, E. P.; Kessler, V. G.; Yanovsky, A. I.; Struchkov, Y. T. *J. Chem. Soc., Chem. Commun.* **1993**, 21–23.
(42) Fischer, R.; Görls, H.; Westerhausen, M. *Inorg. Chem. Commun.* **2005**, *8*, 1159–1161.
(43) Ruspic, C.; Harder, S. *Organometallics* **2005**, *24*, 5506–5508.
(44) Gärtner, M.; Görls, H.; Westerhausen, M. *Organometallics* **2007**, *26*, 1077–1083.
(45) Sobota, P.; Utko, J.; John, L.; Jerzykiewicz, L. B.; Drág-Jarzábek, A. *Inorg. Chem.* **2008**, *47*, 7939–7941.
(46) Green, S. P.; Jones, C.; Stasch, A. *Angew. Chem.* **2008**, *120*, 9219–9223; *Angew. Chem., Int. Ed.* **2008**, *47*, 9079−9083. .
(47) Grimme, S. *J. Comput. Chem.* **2004**, *25*, 1463–1473. (a) Grimme, S. *J. Comput. Chem.* **2006**, *27*, 1787–1799.
(48) Petrie, S *Int. J. Mass Spectrom.* **2003**, *227*, 33–46.
(49) Reddy, A. S.; Zipse, H.; Sastry, G. N. *J. Phys. Chem. B* **2007**, *111*, 11546–11553.
(50) Lin, Y. C.; Williams, D. E. *Acta Crystallogr.* **1975**, *B31*, 318–320.

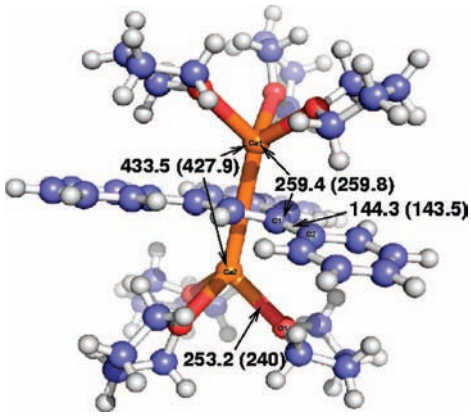

Figure 4. Calculated B97-D triplet structure ($S = 1$) of **2** (Ca orange, O red, C blue, H gray) is given for comparison reasons. Selected distances (in pm) are compared with the experimental values given in parentheses.

Table 1. Selected Bond Distances (pm) of Complex **2** Obtained for DFT Calculations[a]

method	Ca1−Ca2	Ca1−C1	Ca2−O1	C1−C2
B97-D/RI/TZVP ($S = 1$)	435.7	260.7	252.1	144.4
B3LYP/TZVP ($S = 1$)	435.0	261.2	245.3	144.5
TPSS/RI/TZVP ($S = 1$)	430.3	259.9	244.6	144.8
B97-D/RI/TZVPP ($S = 1$)	433.5	259.4	253.2	144.3
TPSS/RI/TZVPP ($S = 1$)	429.2	259.1	246.7	144.9
B97-D/RI/TZVPP ($S = 0$)	424.4	257.0	257.2	145.3
TPSS/RI/TZVP ($S = 0$)	421.0	254.7	248.6	144.7
TPSS/RI/TZVPP($S = 0$)	420.3	254.2	248.3	144.8
experiment	427.9	259.8	240.5	143.5

[a] Note the comparatively small basis set effect; the large TZVPP and the TZVP basis sets yield similar results.

structure), while the open-shell singlet is close in energy; in fact, it is lower in energy by about −30 kJ/mol with about 30 pm shorter bond length than the triplet state (401.9 pm with B97-D). The spin polarization found for the open-shell broken-symmetry singlet state turned out to be rather small.

We consider Grimme's functional to be the appropriate for the study of the large inverse sandwich complex with six THF solvent molecules. However, results from standard density functionals compare surprisingly well, as we shall also see for the large complex. The optimized B97-D triplet structure of the complete solvent-containing complex **2** is presented in Figure 4 and found to be in excellent agreement (note the very slightly tilted phenyl substituents, which break the rotational symmetry). The Ca···Ca distance varies over a wide range depending on the total spin state. The agreement between the experimental and calculated structures is very good for the triplet state. We should note that we found the singlet state of compound **2** to be lower in energy than the triplet state. Since COSMO continuum solvation (see Computational Methodology) reduces this energy gap to a certain extent, we suspect that solvation effects may be the reason for the stabilization of the triplet state in experiment (see next section). In the following, we focus on the triplet state of compound **2** only.

Comparing standard density functionals with the tailored dispersion-corrected functional B97-D, we note that the functionals B3LYP and TPSS yield unexpectedly reliable results (which may be taken as a first indication for ionic bonding in compound **2**). As already noted for the small model Ca−tpb−Ca, the Ca−Ca distance is smallest for the TPSS functional also for compound **2** (Table 1). For comparison we also included the open-shell broken-symmetry singlet state (calculated as a broken-symmetry solution), which features a shorter Ca−Ca distance.

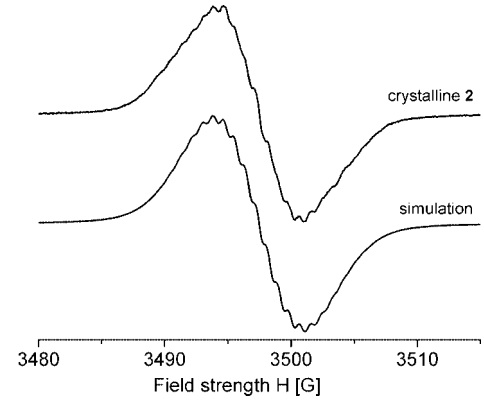

Figure 5. EPR spectrum (X-band) of crystalline **2** at room temperature and the simulated spectrum (half-height width $\Delta H_{pp} = 1.2$ G; Lorentz form; see text).

Properties of Complex 2. Complex **2** is a pyrophoric, extremely air and moisture sensitive solid. The color of a solution of **2** depends on solvent (solvatochromism) and temperature (thermochromism). A THF solution of **2** turned from dark green at −90 °C to deep blue (−40 °C) and blue-violet (−20 °C) and at +20 °C to red-violet. Addition of 18-crown-6 at room temperature led to an apple-green color of the solution. The color is in accord with a small HOMO−LUMO gap (0.24 eV for compound **2** and 0.30 eV for the small model [Ca−tpb−Ca] without solvent molecules; B97-D/TZVP). The ^{1}H NMR spectrum at 400.25 MHz of a [D_8]THF solution showed broad resonances at $\delta = 1.73$ and 3.58 ppm (THF) and at $\delta = 3.25$ (inner arene), 4.58 (*o*-H), 5.80 (*p*-H), and 5.89 ppm (*m*-H). The strong high-field shift of the resonances is a consequence of negative charge, paramagnetism, and metal coordination. Coordination of neutral $(OC)_3Cr$ fragments to the π-system of uncharged tpb also leads to shielded H atoms.[51]

Susceptibility measurements gave 2.33 μ_B which correlates to a spin $S = 1$ (triplet) matched by the quantum chemical calculations. It was shown earlier that 1,3,5-triphenylbenzene can only be reduced to a doubly negative anion even in the presence of a large excess of electropositive metals.[52,53] Also the term scheme predicts a triplet ground state.[52,54]

The EPR spectrum of crystalline **2** is represented in Figure 5. At room temperature (the spectrum shows no obvious dependency on temperature) a completely symmetrical signal of an organic π-radical with the *g*-value of $g = 2.0023$ (*g*-value of the "free" electron) is obtained with a hyperfine pattern of 16 lines. The observed high symmetry of the signal is justified in the existence of two delocalized electrons which interact with the same environment but not with each other. The underlying presence of the C_3-like symmetry of compound **2** is leading to four different types of hydrogen atoms in the intensity ratio of 3 ($H_{inner\text{-}arene}$):6 ($H_{o,o'\text{-}phenyl}$):6 ($H_{m,m'\text{-}phenyl}$):3 ($H_{p\text{-}phenyl}$). Furthermore, the observed hyperfine pattern shows a reduction of the

(51) Mailvaganam, B.; McCarry, B. E.; Sayer, B. G.; Perrier, R. E.; Faggiani, R.; McGlinchey, M. J. *J. Organomet. Chem.* **1987**, *335*, 213–227.
(52) Sommerdijk, J. L.; van Broekhoven, J. A. M.; van Willigen, H.; De Boer, A. *J. Phys. Chem.* **1969**, *51*, 2006–2009.
(53) Broekhoven, J. A. M.; Sommerdijk, J. L.; de Boer, E. *J. Mol. Phys.* **1971**, *20*, 993–1003.
(54) Li, S.; Ma, J.; Jiang, Y. *J. Phys. Chem.* **1997**, *101*, 5587–5592.

theoretical number of lines by effects of superposition. These results were verified and confirmed with the aid of a simulated EPR spectrum (Figure 5) with the following coupling constants derived from the measured spectrum: A ($6H_{o,o'\text{-phenyl}}$) = 1.7 G, A ($6H_{m,m'\text{-phenyl}}$) = 1.7 G, A ($3H_{p\text{-phenyl}}$) = 0.85 G, and A ($3H_{\text{inner-arene}}$) = 0.85 G. The symmetry of the EPR signal confirms that the calcium atoms are only located on the C_3 axis of the tpb^{2-} ligand,[52] whereas the $(OC)_3Cr$ fragment was also bound to the outer phenyl rings.[51]

Reaction Energies, Ionization Energies, and Electron Affinities. The DFT calculations allow us to assign reaction energies to the formation of compound **2** from two neutral Ca atoms, six THF molecules, and the arene ligand. Since B3LYP has been established as some sort of standard functional, we also provide B3LYP/TZVPP results for comparison. The reaction energy at 0 K is then estimated to be −320 kJ/mol exothermic with B97-D/TZVPP (−330 kJ/mol with B3LYP/TZVPP). If the solvation of the Ca atoms is excluded, i.e., if two solvated atoms $Ca(thf)_3$ react with the neutral arene, the energy is still exothermic by −232 kJ/mol with B97-D/TZVPP (−214 kJ/mol with B3LYP/TZVPP). The effect of the solvent molecules on the overall stability is thus quite remarkable. However, if the reaction of two Ca atoms solvated by four THF molecules each with the arene ligand to yield compound **2** plus two liberated THF molecules is considered, the reaction energy is still −200 kJ/mol (B97-D/TZVPP). Of course, it would be desirable to know the *intrinsic* reaction energy of two unsolvated Ca atoms reacted with the neutral arene ligand. This generic reaction is only exothermic by −64 kJ/mol with B97-D/TZVPP (−56 kJ/mol with B3LYP/TZVPP), indicating the prominent role of solvation effects in Ca chemistry. Note that in all these calculations, singlet educts have been chosen to yield the *triplet* product.

We also calculated electron affinities and ionization energies with the COSMO continuum solvation model with B3LYP/TZVPP single-point calculations on B97-D/TZVPP optimized structures in order to understand the energetics of a charge transfer from two Ca atoms onto the tpb ligand. The following set of reaction energies clearly demonstrates that a double single electron transfer is most likely.

$$2Ca^0(THF)_3 + tpb^0(S=0) \rightarrow 2Ca^{1+}(THF)_3 + tpb^{2-}(S=1) \quad [-163\ \text{kJ/mol}]$$

$$\rightarrow \text{Complex } \mathbf{2}\ (S=1) \quad [-174\ \text{kJ/mol}]$$

$$2Ca^0(THF)_3 + tpb^0(S=0) \rightarrow 2Ca^{1+}(THF)_3 + tpb^{2-}(S=0) \quad [-147\ \text{kJ/mol}]$$

$$2Ca^0(THF)_3 + tpb^0(S=0) \rightarrow 2Ca^{2+}(THF)_3 + tpb^{4-}(S=0) \quad [-8\ \text{kJ/mol}]$$

$$Ca^0(THF)_3 + tpb^0(S=0) \rightarrow Ca^{2+}(THF)_3 + tpb^{2-}(S=0) \quad [-130\ \text{kJ/mol}]$$

The total B3LYP/TZVPP formation energy of compound **2** is thus −337 kJ/mol if a COSMO solvation model is employed, which is in excellent agreement with the −330 kJ/mol for the isolated compound **2** (but including six THF molecules, of course) given above.

Bonding Situation in the Inverse Sandwich Complex. The quantum-chemical calculations produced a wave function with occupied molecular orbitals delocalized from one Ca center over the arene to the second Ca ion with notable d-orbital contribution from the metal atomic orbitals.

In order to better understand the bonding in the inverse sandwich complex, we investigated the frontier orbitals. We first studied the lowest three *unoccupied* molecular orbitals of the arene ligand. These were obtained in a spin-restricted B97-D/TZVP calculation. Their antibonding character is easily recognizable in Figure 6. Note the d-type symmetry of the LUMO and LUMO+1 on the central benzene core, which would already be obtained in a simple Hückel MO analysis. Now, these three orbitals should interact with valence atomic orbitals of the two Ca atoms, and in fact, we found that exactly these three orbitals become involved in bonding in the inverse sandwich complex **2**, as Figure 6 shows.

It is important to note that the molecular orbitals of the complex were obtained from a spin-unrestricted calculation of the triplet state. Thus, they are all spin orbitals of α-type. While HOMO and HOMO-1 have no β-orbital analogue, HOMO-2 is also found in the β-series of orbitals. Note that α-HOMO-1 and α-HOMO-2 of the complex are almost degenerate (−1.705 and −1.759 eV, B97-D/TZVP) as much as LUMO+1 and LUMO of the ligand (−2.093 and −2.096 eV, B97-D/TZVP), while α-HOMO of the complex (−0.512 eV) and LUMO of the isolated ligand (−1.350 eV) are higher in energy and α-HOMO-3 is much lower in energy (less than −4 eV).

We see that the four Ca valence electrons occupy the lowest lying ligand orbitals successively. The two lowest energy orbitals of the ligand, LUMO and LUMO+1, become the two lowest energy orbitals of the complex, namely HOMO-2 and HOMO-1, respectively. Then, the LUMO+2 is occupied by one electron to become the α-HOMO of the complex. This also explains why the quintet state is energetically close, as another ligand orbital could be occupied by another electron from the Ca atoms.

While the highest occupied α-molecular orbital is solely dominated by the arene ligand over which it is completely delocalized (thus one electron is completely transferred from the Ca atoms onto the tpb ligand), the HOMO-1 and HOMO-2 already feature interesting orbital overlaps of d-type Ca atomic orbitals with the π-MOs of the arene ligand (describing the partial transfer of additional electron density from the Ca atoms onto the tpb ligand; see population analysis below for detailed partial charge distributions), which are of this symmetry. Hence, the importance of d-functions in the basis set is evident to account for this effect.

Of course, one would have expected the delocalized HOMO in a qualitative picture in which two neutral Ca atoms transfer one electron each into the LUMO of the neutral arene ligand which would then become the HOMO of the complex. While this is partly true in the unrestricted framework, where the LUMO can only be occupied by one electron, the total picture is still valid, as we shall see in the population analysis given below.

A Löwdin population analysis confirmed that both Ca ions carry a positive charge of about 0.6 electrons. Note that 0.6 electrons can be considered as a single positive charge since the TZVPP orbital-decomposition of the charge is not unique. An analogous Mulliken analysis with the TZVPP basis set yields about 1.10 electrons for B97-D and about 1.25 electrons for TPSS. Regarding the carbon atoms of the ligand, the population analysis shows an alternating charge pattern of −0.3 to −0.4 electrons distributed all over the conjugated system. Population analyses hence confirm the charge-separated Ca(I)−arene-(2−)−Ca(I) structure of the complex. The positive charges are almost exclusively localized on the Ca centers, while the doubly negative charge is distributed over the arene ligand. Since

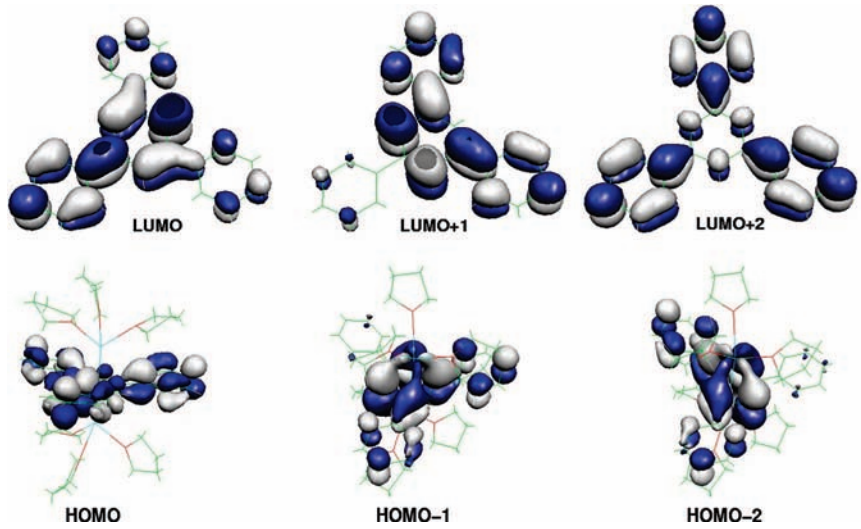

Figure 6. Unoccupied frontier orbitals of the tpb ligand and occupied frontier α-orbitals of the inverse sandwich complex **2**.

Table 2. Crystal Data and Refinement Details for the X-ray Structure Determinations of **1** and the "Inverse" Sandwich Complex **2**

compound	**1**	**2**
formula	$C_{32}H_{33}BrMgO_2$	$C_{48}H_{66}Ca_2O_6$
fw ($g \cdot mol^{-1}$)	553.80	819.17
T/°C	−90(2)	−90(2)
crystal system	orthorhombic	hexagonal
space group	*Pbca*	$P6_3/m$
a/Å	8.7189(2)	14.3116(16)
b/Å	20.6162(5)	14.3116(16)
c/Å	30.8439(6)	13.612(2)
V/Å^3	5544.2(2)	2414.5(5)
Z	8	2
ρ ($g \cdot cm^{-3}$)	1.327	1.127
μ (cm^{-1})	15.32	2.79
measured data	33 922	13 247
data with $I > 2\sigma(I)$	4096	1293
unique data/R_{int}	6343/0.0940	1901/0.0932
wR2 (all data, on F^2)[a]	0.1014	0.3328
R1 ($I > 2\sigma(I)$)[a]	0.0456	0.1057
s[b]	1.004	1.070
res. dens./$e \cdot Å^{-3}$	0.338/−0.476	0.949/−0.654
abs. method	none	none
CCDC no.	706764	692423

[a] Definition of the R indices: R1 = $(\Sigma||F_o| - |F_c||)/\Sigma|F_o|$ wR2 = $\{\Sigma[w(F_o^2-F_c^2)^2]/\Sigma[w(F_o^2)^2]\}^{1/2}$ with $w^{-1} = \sigma^2(F_o^2) + (aP)^2$. [b] $s = \{\Sigma[w(F_o^2 - F_c^2)^2]/(N_o - N_p)\}^{1/2}$.

especially partial charges from Mulliken population analyses are affected by basis set size effects, we should supplement the results discussed so far by a population analysis which is less prone to the choice of basis set. For this we chose the natural population analysis based on natural bond orbitals (NBO) of Weinhold (see Computational Methodology). First, we investigated the charge distribution in the generic (completely unsolvated) small model Ca−tpb−Ca and found a single positive charge on each Ca atom and, consequently, the remaining two negative charges on the tpb ligand. These results are almost independent of density functional and structure as the following data show. For a TPSS/TZVP NBO analysis performed at the TPSS optimized structure, we find charges of +1.03 and +1.02 at the Ca atoms. Single-point NBO calculations on the B97-D structure with BP86/TZVP and B3LYP/TZVP yield charges of +1.01 and +1.04 and of +1.01 and +1.02, respectively. However, a similar analysis with B3LYP/TZVP for the complete (microsolvated) system, i.e., for compound **2**, $(thf)_3Ca$-tpb-$Ca(thf)_3$ produced a 4-fold negative charge (−3.68 au) at the tpb ligand with accompanying 2-fold positive charges on the Ca atoms (+1.91 and +1.78 au). It is important to note that the partial charge of the solvent molecules turns out to be zero and thus all negative charge resides on the tpb ligand. But this charge distribution is in contradiction to the energetical picture, which is strongly in favor of a 2-fold rather than a 4-fold reduction of the tpb ligand. Hence, in view of the general peculiarities of charge decomposition analyses we do not consider the NBO analysis for the microsolvated system to be reliable and refer instead to the generic system for a discussion of the charge distribution, for which all three population analyses yield Ca(I) atoms. The six THF solvent molecules can stabilize a large positive charge on the Ca centers, which is likely to be the reason for the increased partial charges in compound **2**. However, a 4-fold negative charge on the tpb ligand is unlikely for energetical reasons, while at the same time no charge is transferred onto any of the six coordinating solvent molecules.

Conclusion

The important result is that compound **2** consists of two Ca cations and a doubly negatively charged arene ligand. The two calcium atoms are located on the C_3 axis and on opposite sides of the inner arene ring, yielding an inverse sandwich complex. The negative charge is delocalized within the π-system of the arene ligand. This bonding situation is not comparable to the inverted sandwich complex $[(R_2N)_2U(\mu\text{-}\eta^6\text{-toluene})U(NR_2)_2]$ because in this case strong δ-backbonding from uranium(II) into toluene orbitals strongly stabilizes this complex.[55]

The synthesis and isolation of this inverse sandwich complex **2** shows that compounds of alkaline earth metals with the uncommon oxidation state of +1 are stable. Whereas Green, Jones, and Stasch[8] found a procedure to stabilize metal−metal bonds utilizing a shielding periphery of bulky ligands, aromatic ligands with low-lying acceptor orbitals with energies between those of the two ionization potentials of Ca^0 and Ca^+ are also able to stabilize Ca(I) compounds. In both synthetic procedures, however, the atomization energy (lattice energy) of the alkaline earth metals has to be invested. Due to different ionization

(55) Diaconescu, P. L.; Arnold, P. L.; Baker, T. A.; Mindiola, D. J.; Cummins, C. C. *J. Am. Chem. Soc.* **2000**, *122*, 6108–6109.

potentials of magnesium and calcium, the expected Grignard compound **1** is stable whereas we were unable to detect the homologous calcium derivative. Instead of an arylcalcium halide, **2** was isolated with good yield. This compound is extremely sensitive toward moisture and air but shows no tendency to cleave THF. This fact results from the strong reducing power of this compound but delocalization of the negative charge leads to a rather weak Lewis basicity.

Experimental Section

General. All manipulations were carried out using standard Schlenk techniques in an argon atmosphere under strictly anaerobic conditions. 1,3,5-Triphenylbenzene was purchased from Aldrich, and bromo-2,4,6-benzene was prepared from 1,3,5-triphenylbenzene and bromine in tetrachloromethane. Calcium (granules) was used for activation process[35] as purchased from Aldrich without further purification. Rieke magnesium was prepared according to a literature procedure,[56] washed several times with hot acetone, and dried in vacuum at 80 °C. EPR spectra were measured on a Bruker ESP 300 E X-band spectrometer with modulation amplitude of 0.104 G. The EPR spectrum simulations were carried out with the WINEPR SimFonia package from Bruker.

[(2,4,6-(H_5C_6)$_3$$C_6H_2$)MgBr(thf)$_2$] (1). Synthesis. Rieke magnesium (0.24 g, 9.87 mmol) was suspended in 15 mL of THF, and bromo-2,4,6-triphenylbenzene (1.90 g, 4.90 mmol) dissolved in 10 mL of THF was added dropwise over a period of 1 h. The reaction mixture was heated under reflux for 2 h. Thereafter, the solution was cooled to room temperature (rt) and filtered. Reduction of the volume to 8 mL and storage at −20 °C led to precipitation of large colorless needles. Separation and gently drying in vacuum gave 1.72 g (3.10 mmol, 63%) of **1**.

Physical Data for 1. Mp 165 °C. Elemental analysis ($C_{32}H_{33}BrMgO_2$, 553.83): Calcd: Mg 4.39; found: Mg 4.31. ^{1}H NMR (400.25 MHz, 25 °C, [D$_8$]THF): δ 1.79 (8H, m, CH_2, thf), 3.63 (8H, m, CH_2O, thf), 7.29 (3H, m, $^3J_{H-H}$ = 8.0 Hz, *p′*/*p″*-C*H*), 7.37 (2H, t, $^3J_{H-H}$ = 7.6 Hz, *m″*-C*H*), 7.48 (4H, t, $^3J_{H-H}$ = 7.6 Hz, *m′*-C*H*), 7.66 (2H, s, *m*-C*H*), 7.79 (4H, d, $^3J_{H-H}$ = 7.4 Hz, *o′*-C*H*), 7.94 (2H, d, $^3J_{H-H}$ = 7.2 Hz, *o″*-C*H*). ^{13}C {^{1}H} NMR (100.65 MHz, 25 °C, [D$_8$]THF): δ 27.3 (4C, *C*H$_2$, thf), 67.8 (4C, *C*H$_2$O, thf), 124.5 (2C, *m*-CH), 125.5 (2C, *o″*-CH), 126.6 (1C, *p″*-CH), 127.6 (2C, *p′*-CH), 127.9 (4C, *m′*-CH), 128.2 (2C, *m″*-CH), 129.5 (4C, *o′*-CH), 139.5 (1C, *i″*-*C*), 143.4 (1C, *p*-*C*), 150.6 (2C, *i′*-*C*), 154.2 (2C, *o*-*C*H), 164.1 (1C, *i*-*C*). IR (Nujol, KBr, cm^{-1}): 2930 vs(br.), 1966 m, 1950 m, 1904 w, 1883 w, 1829 w, 1809 w, 1766 m, 1594 s, 1575 m, 1520 m, 1457 vs, 1411 s, 1380 vs, 1347 m, 1310 m, 1250 m, 1230 m,1179 m, 1155 m, 1115 m, 1076 s, 1029 s, 989 m, 913 s, 873 s, 752 vs, 725 s, 698 vs, 626 m, 610 s. MS (FAB, *m*/*z*, [%]): 480 (M − thf) [10], 408 (M − 2thf) [22], 306 (tpb) [100]. For the NMR assignments, atoms in the central ring are unprimed, atoms in the ortho phenyl groups are primed, and atoms in the para phenyl group are doubly primed.

[(thf)$_3$Ca{μ-(C_6H_5)$_3$$C_6H_3$}Ca(thf)$_3$] (2). Procedure A. Calcium (1.00 g, 24.95 mmol) was activated and dried according to standard procedures and suspended in 50 mL of THF. A solution of bromo-2,4,6-triphenylbenzene (2.71 g, 7.03 mmol) in 10 mL of THF was added at −78 °C. Thereafter, the mixture was shaken for 5 h at −60 °C. The resulting blue solution (showed more than stoichiometric basicity after hydrolysis) was filtered at −40 °C through a Schlenk frit, which was covered with diatomaceous earth. Cooling of this solution to −78 °C afforded the precipitation of black crystals, which were collected and redissolved in 30 mL of THF. The solution was filtered again and storage at −40 °C led to precipitation of black, pyrophoric, and extremely air and moisture sensitive crystals of **2** (1.97 g, 2.40 mmol, 34%). The mother liquor exhibited enormous basicity, and further concentration of the solution resulted in a black powder. Total yield: 4.93 g, 6.02 mmol, 86% (with respect to $Ph_3C_6H_2$-Br).

Procedure B. Calcium (1.00 g, 24.95 mmol) was activated and dried according to standard procedures and suspended in THF (50 mL). A solution of 1,3,5-triphenylbenzene (2.29 g, 7.47 mmol) and bromo-2,4,6-triphenylbenzene (0.32 g, 0.83 mmol) in 10 mL of THF was added at −78 °C. Thereafter, the mixture was shaken for 5 h at −60 °C. The resulting blue solution (which showed enormeous basicity after hydrolysis) was filtered at −40 °C through a Schlenk frit, which was covered with diatomaceous earth. A similar workup procedure as described for procedure A yielded 3.27 g of **2** (3.99 mmol, 53%). The mother liquor still showed significant basicity, and further concentration of the solution gave a black powder. Total yield: 5.56 g, 6.79 mmol (91% with respect to tpb; 82% with respect to tpb and $Ph_3C_6H_2$-Br).

Physical data of 2. Decomposition above 71 °C. Elemental analysis ($C_{48}H_{66}Ca_2O_6$, 819.08): Calcd: Ca 9.77; found: Ca 8.90 (ICP-OES, after treatment with concd HNO_3). ^{1}H NMR ([D$_8$]THF, 400.25 MHz, 300 K): δ 1.73 (CH_2, thf), 3.25 (3H, s, *o′*-H, $\omega_{1/2}$ = 21.69 Hz), 3.58 (CH_2O, thf), 4.58 (6H, s, *o*-H, $\omega_{1/2}$ = 27.10 Hz), 5.80 (3H, s, *p*-H, $\omega_{1/2}$ = 18.98 Hz), 5.89 (6H, s, *m*-H, $\omega_{1/2}$ = 21.69 Hz). ^{13}C{^{1}H} NMR ([D$_8$]THF, 50.32 MHz, 300 K): δ 25.2 (*C*H$_2$, thf), 67.3 (*C*H$_2$O, thf), 98.2 (3C, br., *o′*-C), 114.5 (6C, br., *o*-C), 120.2 (6C, *m*-C), 124.7 (3C, *p*-C), 155.1 (3C, *i*-C), 156.4 (3C, *i′*-C). MS (EI, *m*/*z*, [%]): 306 [100] (tpb), 91 [43] (tropyl), 77 [65] (Ph), 72 [35] (thf). IR (Nujol, KBr, cm^{-1}): 2924 vs, 2854 vs, 1595 m, 1497 m, 1459 s, 1412 m, 1377 m, 1076 w, 1032 w, 873 w, 764 m, 751 m, 701 m, 611 w. Susceptibility measurements (Gouy magnetic balance, 303 K): χ_v = 1.766 10^{-6}, χ_g = 3.247 10^{-6} cm^3 g^{-1}, χ_m = 2.659 10^{-3} cm^3 mol^{-1}, μ_{eff} = 2.33 μ_B ESR (solid, 298 K) g = 2.0023. The extremely large air and moisture sensitivity of compound **2** in solution and the high extinction coefficient prevented its quantitative analytical characterization via UV/vis techniques. For this reason the observed thermochromism of the THF solution was described qualitatively by resulting colors: dark green (183 K), deep blue (233 K), blue-violet (253 K), and red-violet (293 K).

Structure Determinations. The intensity data for compounds **1** and **2** were collected on a Nonius KappaCCD diffractometer using graphite-monochromated Mo Kα radiation. Data were corrected for Lorentz and polarization effects but not for absorption effects.[57,58] The structure was solved by direct methods (SHELXS)[59] and refined by full-matrix least-squares techniques against F_o^2 (SHELXL-97).[60] The hydrogen atoms on C3 and C5 of **1** were located by difference Fourier synthesis and refined isotropically. All other hydrogen atoms were included at calculated positions with fixed thermal parameters. All nondisordered, non-hydrogen atoms were refined anisotropically.[60] POVRAY and XP (SIEMENS Analytical X-ray Instruments, Inc.) were used for structure representations.

Computational Methodology. The all-electron calculations (DFT and MP2) were performed with the quantum chemical program package Turbomole.[61−64] In the DFT calculations we applied Grimme's B97-D functional[39] but also tested the BP86, TPSS, and B3LYP functionals.[65−69] In all calculations the resolu-

(56) Rieke, R. D.; Xiong, H. *J. Org. Chem.* **1991**, *56* (9), 3109–3118.
(57) COLLECT, Data Collection Software; Nonius B. V., Netherlands, 1998.
(58) Processing of X-Ray Diffraction Data Collected in Oscillation Mode: Otwinowski, Z.; Minor, W. in Carter, C. W.; Sweet, R. M. (eds.): *Methods in Enzymology, Vol. 276, Macromolecular Crystallography, Part A*; Academic Press: New York, 1997; pp 307−326.
(59) Sheldrick, G. M. *Acta Crystallogr., Sect. A* **1990**, *46*, 467–473.
(60) Sheldrick, G. M. *SHELXL-97 (Release 97-2)*; University of Göttingen: Göttingen, Germany, 1997.
(61) Ahlrichs, R.; Bär, M.; Häser, M.; Horn, H.; Kölmel, C. *Chem. Phys. Lett.* **1989**, *162*, 165–169.
(62) Møller, C.; Plesset, M. S. *Phys. Rev.* **1934**, *46*, 618–622.
(63) Haase, F.; Ahlrichs, R. *J. Comput. Chem.* **1993**, *14*, 907–912.
(64) Weigend, F.; Häser, M.; Patzelt, H.; Ahlrichs, R. *Chem. Phys. Lett.* **1998**, *294*, 143–152.
(65) Becke, A. D. *Phys. Rev. A* **1988**, *38*, 3098–3100.
(66) Perdew, J. P. *Phys. Rev. B* **1986**, *33*, 8822–8824.
(67) Tao, J.; Perdew, J. P.; Staroverov, V. N.; Scuseria, G. E. *Phys. Rev. Lett.* **2003**, *91*, 146401.

tion-of-the-identity ('RI') density fitting technique in order to speed up the calculations without loss of accuracy. We employed the TZVP and TZVPP basis sets based on the work by Schäfer et al.[70] as implemented in Turbomole. For the calculation of local spin values and partial charges, we applied a modified Löwdin analysis.[71] Details on its implementation into the Turbomole program package can be found in the literature.[72] To assess the role of solvent effects, we employed a continuum model, namely the COSMO model, to account for a THF environment. These calculations have been carried out with the default COSMO parameters of the TURBOMOLE/COSMO implementation. The optimized atomic COSMO radii[73,74] were used. The molecular structures were visualized with the program Molden[75] and the orbitals with the program Molekel.[76]

An important point that should be noted with respect to the accuracy of the calculations is the choice of the one-electron basis set. It turned out that d-type basis functions are absolutely essential for accurate quantum chemical calculations of any kind. While the Ca TZVP basis set of Turbomole 5.10, which we employed here throughout, contains one contracted d-function (out of three primitives) and another primitive d-function, this is *not* the case for the "same" TZVP basis in Turbomole 5.7, which does not contain any d-function. Structure optimization with the latter produces gave Ca−Ca distances that are about 35 pm too large compared to those with the former one. The d-type basis functions are also essential to guarantee orbital overlap with low-lying molecular fragment orbitals of the arene ligand. Hence, d-functions *must not* be neglected; they are more decisive than the chosen method for the electronic structure calculation discussed now. For the calculation of partial charges also the natural population analysis as implemented in Gaussian03 was employed.[77]

Acknowledgment. We thank the Deutsche Forschungsgemeinschaft (DFG, Bonn/Germany) and the Schweizer National-Fonds (Project No. 200021-113479) for generous financial support of this research initiative. We also gratefully acknowledge the funding of the Fonds der Chemischen Industrie (Frankfurt/Main, Germany). S.K. is very grateful to the Verband der Chemischen Industrie (VCI/FCI) for a Ph.D. grant. In addition, we thank Dr. W. Poppitz (MS, GC), Dr. M. Friedrich (NMR, EPR), Prof. G. Kreisel (electrochemistry), Dr. D. Merten (ICP-OES), Dr. H. Breitzke, and Prof. G. Buntkowsky (solid state NMR) for their support.

Supporting Information Available: CIF files giving data collection and refinement details, as well as positional coordinates of all atoms. This material is available free of charge via the Internet at http://pubs.acs.org.

JA808524Y

(68) Becke, A. D. *J. Chem. Phys.* **1993**, *98*, 5648–5652.
(69) Lee, C.; Yang, W.; Parr, R. G. *Phys. Rev. B* **1988**, *37*, 785–789.
(70) Schäfer, A.; Huber, C.; Ahlrichs, R. *J. Chem. Phys.* **1994**, *100*, 5829–5835.
(71) Clark, A. E.; Davidson, E. R. *J. Chem. Phys.* **2001**, *115*, 7382–7392.
(72) Herrmann, C.; Reiher, M.; Hess, B. A. *J. Chem. Phys.* **2005**, *122*, 034102.
(73) Klamt, A.; Eckert, F. *Fluid Phase Equilib.* **2000**, *172*, 43–72.
(74) Sillanpää, A. J.; Aksela, R.; Laasonen, K. *Phys. Chem. Chem. Phys.* **2003**, *5*, 3382–3393.
(75) Schaftenaar, G.; Noordik, J. H. *J. Comput.-Aided Mol. Design* **2000**, *14*, 123–134.
(76) http://www.cscs.ch/molekel/.
(77) Frisch, M. J.; *Gaussian03, Revision B.05*; Gaussian, Inc.: Pittsburgh, PA, 2003.